ARMY RESEARCH LABORATORY

Macroscopic Modeling of $A_3B_{15}A_3$ Triblock Copolymers in B Solvent

by Tanya L. Chantawansri, Jan W. Andzelm, and Joseph L. Lenhart

ARL-TR-5395 **November 2010**

NOTICES

Disclaimers

The findings in this report are not to be construed as an official Department of the Army position unless so designated by other authorized documents.

Citation of manufacturer's or trade names does not constitute an official endorsement or approval of the use thereof.

Destroy this report when it is no longer needed. Do not return it to the originator.

Army Research Laboratory
Aberdeen Proving Ground, MD 21005

ARL-TR-5395 **November 2010**

Macroscopic Modeling of $A_3B_{15}A_3$ Triblock Copolymers in B Solvent

Tanya L. Chantawansri, Jan W. Andzelm, and Joseph L. Lehnart
Weapons and Materials Research Directorate, ARL

REPORT DOCUMENTATION PAGE	Form Approved OMB No. 0704-0188

1. REPORT DATE *(DD-MM-YYYY)*	2. REPORT TYPE	3. DATES COVERED (From - To)
November 2010	Final	

4. TITLE AND SUBTITLE
Macroscopic Modeling of $A_3B_{15}A_3$ Triblock Copolymers in B Solvent

5a. CONTRACT NUMBER

5b. GRANT NUMBER

5c. PROGRAM ELEMENT NUMBER

6. AUTHOR(S)
Tanya L. Chantawansri, Jan W. Andzelm, and Joseph L. Lenhart

5d. PROJECT NUMBER

5e. TASK NUMBER

5f. WORK UNIT NUMBER

7. PERFORMING ORGANIZATION NAME(S) AND ADDRESS(ES)
U.S. Army Research Laboratory
ATTN: RDRL-WMM-G
Aberdeen Proving Ground, MD 21005

8. PERFORMING ORGANIZATION REPORT NUMBER
ARL-TR-5395

9. SPONSORING/MONITORING AGENCY NAME(S) AND ADDRESS(ES)

10. SPONSOR/MONITOR'S ACRONYM(S)

11. SPONSOR/MONITOR'S REPORT NUMBER(S)

12. DISTRIBUTION/AVAILABILITY STATEMENT
Approved for public release; distribution unlimited.

13. SUPPLEMENTARY NOTES

14. ABSTRACT
We have performed dynamic density functional theory calculations for an ABA triblock copolymer immersed in a B-attractive solvent. The triblock copolymer was parameterized for poly[styrene-b-(ethylene-co-butylene)-b-styrene] (SEBS), while the solvent was parameterized for the hydrocarbon oil tetradecane (C_{14}). The effect of the solvent concentration and SEB interaction on the morphology was studied. For a 50/50 vol.% mixture of polymer/solvent, we also considered the effect of solvent molecular weight on the morphology, where we observed a transition between micro- and macro-phase separation at a critical molecular weight. Lastly, elastic properties were calculated using a finite-element based mechanical homogenization method.

15. SUBJECT TERMS
Thermoelastic gels, computational modeling, gels

16. SECURITY CLASSIFICATION OF:			17. LIMITATION OF ABSTRACT	18. NUMBER OF PAGES	19a. NAME OF RESPONSIBLE PERSON
a. REPORT	b. ABSTRACT	c. THIS PAGE			Tanya L. Chantawansri
Unclassified	Unclassified	Unclassified	UU	24	19b. TELEPHONE NUMBER (*Include area code*) (410) 278-2777

Standard Form 298 (Rev. 8/98)
Prescribed by ANSI Std. Z39.18

Contents

List of Figures

Acknowledgements

Tanya L. Chantawansri was supported in part by an appointment to the Postgraduate Research Participation Program at the U.S. Army Research Laboratory (ARL), administered by the Oak Ridge Institute for Science and Education through an interagency agreement between the U.S. Department of Energy and ARL. Calculations were performed on the Department of Defense (DoD) High Performance Computing site at ARL. We would like to thank Drs. M. Berg, F. Beyer, R. Mrozek, K. Stokes, P. Chung, and B. Henz for useful discussion.

INTENTIONALLY LEFT BLANK.

1. Introduction

There is substantial interest in block copolymers due to its tailorability, where morphology can be easily manipulated through four factors: monomer type, polymer architecture, system composition, and molecular size. Important quantities, such as mechanical and physical properties, are influenced by the phase morphology and are essential when determining potential applications (*1*). Due to the large parameter space associated with block copolymers, computational modeling can be used to determine the relevant parameters associated with the desired phase behavior in order to speed up the material design process.

One system of interest is in thermoplastic elastomer (TPE) gels composed of triblock or multiblock copolymers immersed in a midblock-selective solvent. The copolymer is composed of a rubbery midblock and short glassy end blocks, where the latter can cluster together to form microdomains, which act as physical crosslink sites situated in a continuous matrix composed of the midblock (*2*). Some examples of TPEs are poly[styrene-butadiene-styrene] (SBS), poly[styrene-isoprene-styrene] (SIS), poly[styrene-isobutylene-styrene] (SIBS), and poly[styrene-(ethylene-co-butylene)-styrene] (SEBS) (*3*). Out of these three, there is particular interest in SEBS, which is the hardest and most resilient against degradation, and is used in a variety of applications such as biomimetic gels, adhesives, sealants, coatings, shoe soles, car parts, and wire insulation (*3*).

While computational modeling is ideal for investigating the block-copolymer morphology, minimal research has been performed on TPE gels. Computationally, this gel can be modeled as an ABA triblock immersed in a B-selective solvent. In this framework, Kim et al. (*4*) used grand canonical Monte Carlo to study the shape, size, distribution, and internal structures of micelles formed at low polymer volume fractions. Mechanical behavior of the micellar phase was also studied by Sliozberg et al. (*5*) using dissipative particle dynamics. For a highly solvated system (80–90 vol.%) Shull and coworkers (*6*) used the unit cell approximation in self-consistent field theory to study the effect of the triblock copolymer midblock length and temperature on the micellar size, geometry, aggregation number, bridging fraction, solvent osmotic pressure, and form factor. Although insight into TPE gels has been gained through these studies, they are limited to systems with high solvent concentrations. For a slightly different system of poly[propylene oxide-ethylene oxide-propylene oxide] triblock in aqueous solution, where the solvent has a slight attraction towards the midblock, Fraaijie and coworkers (*7*) presented select morphologies for a few polymer-solvent compositions. Even so, we are interested in a more comprehensive study for systems where the solvent has a strong selectivity towards the midblock.

We have used the dynamic density functional theory (DDFT) to study the phase behavior of SEBS and the midblock selective hydrocarbon oil tetradecane (C_{14}) as a function of solvent volume fraction and the S-EB interaction parameter, which is inversely proportional to the temperature. Additional calculations for the spherical morphology (at 50/50 vol.% SEBS/C_{14}) were performed to determine the effect of the solvent molecular weight on the phase morphology. Lastly, using a finite-element based mechanical homogenization method for linear elasticity, we have also calculated the Young's and shear moduli for select morphologies.

2. Models and Methods

A polymer gel exhibits both thermal and environmental stability, and possesses enhanced mechanical properties due to its ability to form physical crosslinks where the triblock copolymers bridges two microdomains. In this particular study, the phase behavior of SEBS in C_{14} is studied using DDFT, which was developed by Fraaije et al. (*8, 9*). The input parameters required by the method are the number of beads and the polymer interaction parameters, which can be related to the solubility parameters. The SEBS of interest is manufactured by Kraton Polymers under the label Kraton G1652M, and is composed of 29.0 to 30.8 wt.% styrene with a molecular weight of about 99,000 g/mol. Although numerous methods are available to calculate solubility parameters, we chose to use group additive methods through the SYNTHIA (*10*) module of Material Studios (MS), which uses the Fedors predictions of the solubility parameters. Both of the rubbery components and the midblock selective C_{14} exhibit similar values of 17.53 $\sqrt{(J/cm^3)}$, 17.1 $\sqrt{(J/cm^3)}$, and 17.53 $\sqrt{(J/cm^3)}$ for ethylene, butylene, and tetradecane, respectively, which indicate that they are miscible within each other relative to the styrene block (20.1 $\sqrt{(J/cm^3)}$). Thus, the ethylene-co-butylene midblock and the C_{14} solvent can be represented as the same molecule, where the SEBS and C_{14} blend are modeled as $A_3B_{15}A_3 + B_1$. In this discretization, the styrene block contributes about 28% of the SEBS volume and assuming an average density, molecular volume, and molecular mass of 0.92 g/cm^3, 48.9 cm^3/mol, and 42.08 g/mol, respectively, for ethylene-butylene and 1.05 g/cm^3, 97.0 cm^3/mol, and 104.2 g/mol, respectively, for styrene, each bead is calculated to occupy a volume of approximately 5100 cm^3/mol, where each styrene and ethylene-butylene bead contains 53 and 105 monomers, respectively. The solvent is also represented using the same bead volume, which corresponds to 23 molecules of C_{14}.

The MESODYN module through the commercial software MS (*10*) was used to develop a phase diagram for SEBS + C_{14} for different volume fractions of the solvent, Φ_s and the A-B interaction parameters, ε_{AB} or χ_{AB}. MESODYN uses an interaction parameter ε_{AB} to characterize the repulsion between the A and B species, which is inputted into the program as the quantity ε_{AB}/ν, where ν is the mean field excluded volume parameter. This interaction parameter is related to the Flory Huggins parameter χ_{AB} through $\chi_{AB} = [2\varepsilon_{AB} - \varepsilon_{AA} - \varepsilon_{BB}]/(2\nu kT)$ (*8, 11*). In addition to the

composition of the triblock and the interaction parameter, the degree of polymerization, N, is also an important parameter since the entropy of mixing is dependent on the size of the polymer. To capture this contribution an effective repulsion parameter, $\chi_{AB}N$, is defined, which is calculated for our system through $\chi_{AB}N \approx 7.82\ \varepsilon_{AB}/\nu$ mol/kJ, where we consider a temperature of T=323K and zero self-interaction parameters $\varepsilon_{AA} = \varepsilon_{BB} = 0$.

The simulations were performed on a periodic cubic simulation box with 32x32x32 grid points using the recommended MESODYN parameters for the grid spacing, noise, compressibility parameter, and Crank-Nicholson tolerance. The simulation box was sheared normal to the *y*-direction at a rate of 5.000 e-3, 5.000e-2, and 1.000e-2, for 9,000 time steps after 5,000 time steps of equilibrium, followed by 12,000 time steps of equilibration, where each time step is 50 ns. Shearing was performed to speed up phase separation and as a mechanism to escape from metastable configurations, where the free energy of each phase before (at 5,000 time steps) and after (at 26,000 time steps) shearing are compared for the three shear rates. The phase with the lowest free energy was then considered the equilibrium morphology. This is similar to the method used by Zvelindovsky for the spherical morphology for an AB polymer melt and ABA block copolymer and solvent mixture (*12*). Although shear transforms the phase morphology into the cylindrical phase, the cylinders can break or deform to different morphologies such as the spherical or gyroid phase during the equilibrium period following the shearing process. This reordering reduces the packing frustration associated with being constrained to a highly energetically unfavorable configuration. Simulations were performed for Φ_s ranging from 0 to 0.9 in increments of 0.1, where ε_{AB}/ν was varied from 4 kJ/mol to 14 kJ/mol in increments in 0.2 kJ/mol.

3. Results and Discussion

The phase diagram produced using DDFT for SEBS + C_{14} system is shown in figure 1, where we observed three classical microphases: gyroid, cylindrical, and spherical. Although the phase diagram was produced to describe our system of interest, it can be used as a universal phase diagram for any $A_3B_{15}A_3 + B_1$ system. The interaction parameter can be calculated for an experimental system using the equation, $\chi_{AB} = V_{ref}[\delta_A - \delta_B]^2/(RT)$ (*13, 14*), where δ_A and δ_B is the solubility parameters of species A and B, respectively, and V_{ref} is a reference molar volume.

Morphologies obtained using MESODYN are typically defective and metastable, where defect-free configurations are very difficult to obtain (*9*). Although shearing can be used to escape from metastable morphologies, obtaining ordered structures is still challenging. Nevertheless, the morphologies can still be differentiated into three microstructures: spheres, cylinders, and gyroid. In our simulations, it is difficult to discern between spheres arranged in BCC symmetry and a liquid micellar phase, which are stable at low and high solvent dilution (*15*), respectively, therefore they will not be differentiated in this study.

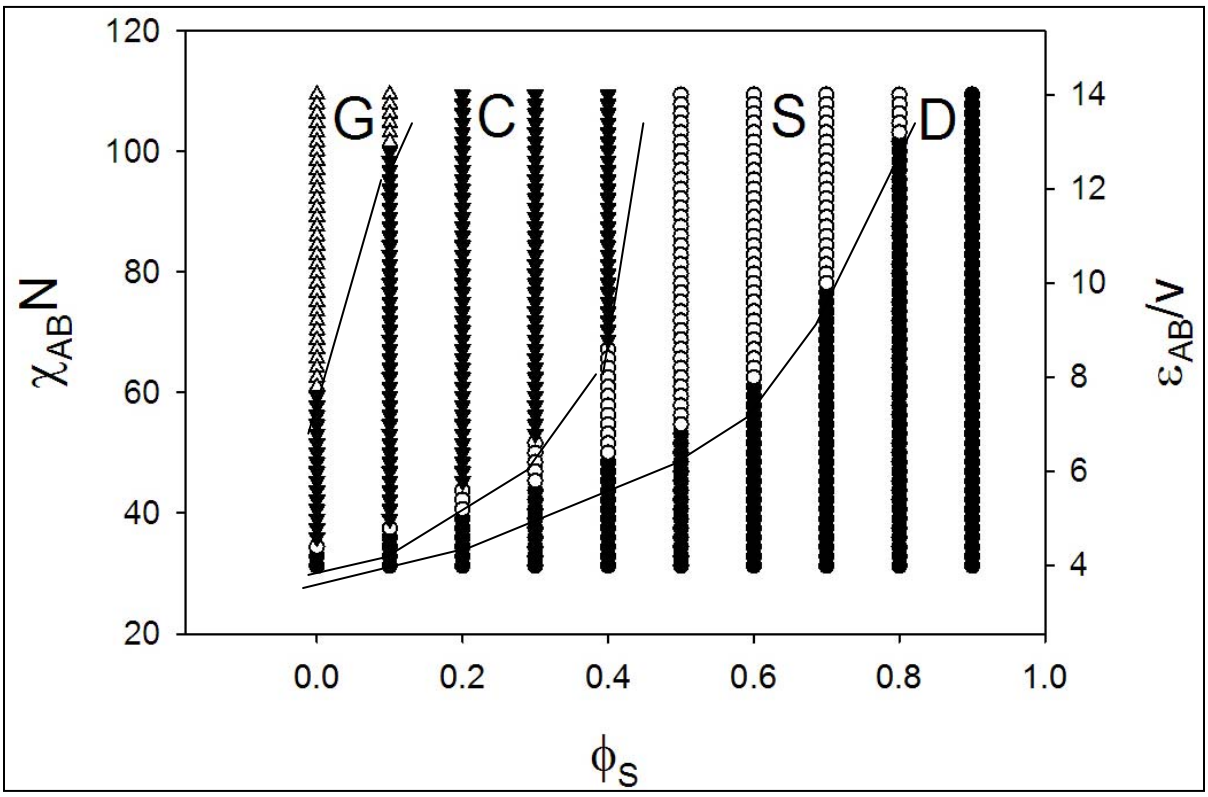

Figure 1. Phase diagram produced using DDFT for an ABA triblock and B-selective solvent. The lines are drawn to guide the eyes and are not actual phase boundaries. G, C, S, and D represent the gyroid, cylindrical, spherical, and disorder phases, respectively.

For the neat ABA triblock copolymer system ($\Phi_s = 0$), the phase sequence (disorder → spherical → cylindrical → gyroid) is observed with an increasing interaction parameter or decreasing temperature. This is the same sequence that was obtained using self-consistent field theory for a symmetric (A blocks equal in length) triblock by Matsen and Thompson (*16*) at approximately the same A volume fraction. At this volume fraction, they observed a $\chi_{AB}N \approx 13$ associated with the order-disorder transition (ODT) for a triblock copolymer of length 2N(16). We observe a similar value, $\chi_{AB}N \approx 17$, after the doubling of the triblock copolymer N is accounted for. This deviation along with shifts in the phase boundaries were also observed by Horvat et al. (*11*); they were attributed to the small number of beads used to resolve the chain and the nonlocality of the non-ideal interactions. In addition, the DDFT method includes a random noise term in the equations associated with the density evolution, which the self-consistent field theory (SCFT) lacks. Although the noise is not capable of extending the theory beyond the mean field approximation (*17*), it may shift the ODT to slightly higher values of $\chi_{AB}N$.

Several experimental and theoretical studies have shown that the thermodynamic behavior of a symmetric ABA triblock is very similar to that of a corresponding AB diblock system obtained by snipping the triblock in half. This is because the entropy gain through this snipping is relatively small, which allows the phase behavior for the neat triblock to be governed by the

same principles (*16, 18–20*). Due to the asymmetric of the snipped triblock copolymer (A_3B_7), competition between the A and B stretching energies stabilize morphologies with curved interfaces and the lamellar phase is energetically unfavorable as the A volume fraction deviates from 0.5 (*16, 12, 22*). The sequence of the curved morphologies observed for our system is due to a delicate balance between interfacial tension and chain stretching, where the former and latter contributions dominate at high and low $\chi_{AB}N$, respectively. At low segregation or at high temperatures, the disorder phase is stable since the repulsion between the A and B segments is weak and entropy dominates. Upon cooling a disordered phase, a first order transition to the spherical morphology occurs. Due to the asymmetry exhibited by A_3B_7, the system favors morphologies with a higher interfacial curvature, such as the spherical phase at high temperatures, where the majority component is allowed to relax at the expense of the minority block (*23*). This order-order transition was first predicted by Leibler (*24*) for an AB diblock copolymer using Landau theory and since then has been studied theoretically and experimentally (*25*) for numerous block copolymer systems. An order-order transition to the cylindrical phase occurs when $\chi_{AB}N$ is further increased and the enthalpic contribution becomes more significant. In this situation, the spheres deform and coalescence together to form cylinders arranged in a hexagonal lattice due to thermodynamic instability of the spherical interface, where the reduction in interfacial area lowers the enthalpic contribution to the free energy (*26, 27*). When the enthalpic contribution begins to dominate at large $\chi_{AB}N$, the gyroid phase becomes stable where the geometry is capable of producing interfaces of uniform curvature while retaining domains of uniform thickness (*16*).

Adding solvent into the system not only stabilizes the cylindrical and/or spherical morphology, but also delays microphase separation where the value of $\chi_{AB}N$ associated with the ODT is shifted to higher values. As seen in figure 1, the value of $\chi_{AB}N$ at which the disorder phase transforms into the spherical morphology increases with increasing solvent concentration and is due to the large entropy of mixing gained by distributing the solvent molecules randomly within the system (*28*). For very low volume fractions of solvent, $\Phi_s = 0.1$, the same phase sequence (disorder → spherical → cylindrical → gyroid) as seen in the neat triblock is observed, where the concentration of the solvent is not large enough to destabilize this progression. Further increasing the solvent concentration from $\Phi_s \approx 0.2$ to $\Phi_s \approx 0.4$, destabilizes the gyroid morphology, while contracting and enlarging the window of stability for the cylindrical and spherical phase, respectively, with increasing solvent concentration. For $\Phi_s \approx 0.5$ to $\Phi_s \approx 0.8$, only the spherical morphology is observed, where microphase separation does not occur at higher solvent volume fractions. The phase sequence observed at $\Phi_s \approx 0.5$, spherical → disorder, with increasing temperature was also verified experimentally by Sugimoto et al. (*29*).

This phase behavior observed in figure 1 can be explained using the trajectory approach described by Hanley et al. (*30*) and Suo et al. (*30, 31*). With increasing solvent concentration, we observe a phase transition (horizontal trajectory) from the gyroid → cylindrical → spherical → disorder at high A-B repulsion (*16*), which is the same phase sequence that is observed for a neat

triblock copolymer when the B volume fraction is increased from ~70 vol.%. This is due to the B-selective solvent, which swells the B domain and modifies the relative concentration of the A and B blocks such that the effective B volume fraction increases compared to the pure triblock copolymer system (*31, 32*). When the solution is heated ($\chi_{AB}N$ decreases), the phase sequence can be determined by a diagonal trajectory towards structures dictated by the block copolymer A fraction since the solvent becomes less selective (*30, 33*). This diagonal trajectory, applied to the neat copolymer phase diagram, produces the correct phase sequence upon heating for the solution: cylindrical → spherical → disorder and spherical → disorder at intermediate and high solvent dilutions, respectively.

The morphology of the ABA + B blend is influenced by the length of the midblock selective solvent. Up to now the solvent has been modeled as a single B bead, but as the molecular weight of the solvent increases, additional beads can be used to represent the solvent. As the number of beads increase, the solvent becomes a homopolymer and chain stretching becomes an important contribution in determining the equilibrium morphology. Due to this extra interplay, there will a transition between microphase and macrophase separation with increasing solvent molecular, which we observed for our gel system. We considered a 50/50 blend (by volume) of the $A_3B_{15}A_3$ triblock and B homopolymer-solvent, since the spherical morphology was verified by both our model and experimentally (*29*) for a low molecular weight solvent. For this system, we studied the phase evolution for three interaction parameters, $\chi_{AB}N$ = 46.9, 59.4, 73.5, as a function of increasing homopolymer-solvent bead length or equivalently molecular weight. At a low interaction parameters of $\chi_{AB}N$ = 46.9, where our $A_3B_{15}A_3$ and B_1 system is initially disordered (figure 2a), we begin to observe the onset of phase separation to a spherical phase when the length of the homopolymer-solvent is increased to 3 beads (figure 2b) and to an ordered spherical phase at 5 beads (figure 2c). Macrophase separation is observed when the homopolymer-solvent is equal to 7 beads (figure 2d), where a disordered phase composed of mostly the homopolymer-solvent coexists with a cylindrical microphase. Similar behavior is observed for larger interaction parameters such as $\chi_{AB}N$ = 59.4 or $\chi_{AB}N$ = 73.5, where the A-B repulsion is substantial enough to microphase separate the original $A_3B_{15}A_3$ and B_1 system into the spherical morphology (figure 3a). At these two interaction parameters, macrophase separation occurs when the homopolymer-solvent is represented by 5 and 4 beads at $\chi_{AB}N$ = 59.4 or $\chi_{AB}N$ = 73.5, respectively (figure 3b). Variations in the number of beads associated with macrophase separation are due to the increased contribution of interfacial energy to the overall free energy with increasing interaction parameter. Since the majority of the homopolymer-solvent is expelled from the triblock copolymer when macrophase separation is observed, the triblock microphase separates into the morphology associated with the neat $A_3B_{15}A_3$ triblock. This is not observed at $\chi_{AB}N$ = 73.5, where the neat $A_3B_{15}A_3$ triblock takes the gyroid morphology. This discrepancy may be due to packing frustrations associated with this geometry, where residual homopolymer-solvent in the microphase can stabilize the cylindrical phase.

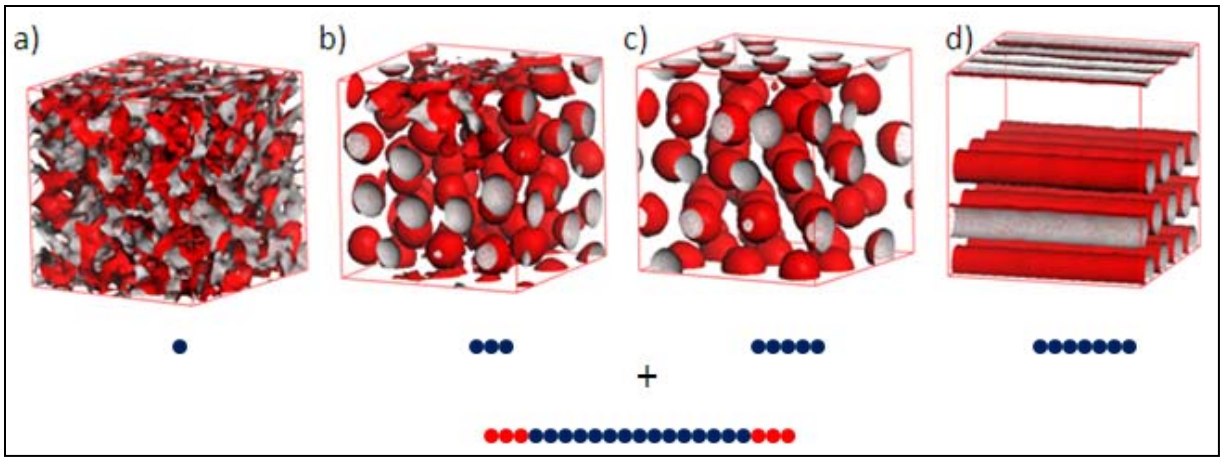

Figure 2. Phase evolution with increasing B homopolymer-solvent length for a 50/50 blend (by volume) of the triblock copolymer and homopolymer-solvent for $\varepsilon_{AB}/\upsilon = 6.0$ or $\chi_{AB}N = 46.9$. Isosurfaces are shown for the A component (red online), where the B component is excluded for clarity.

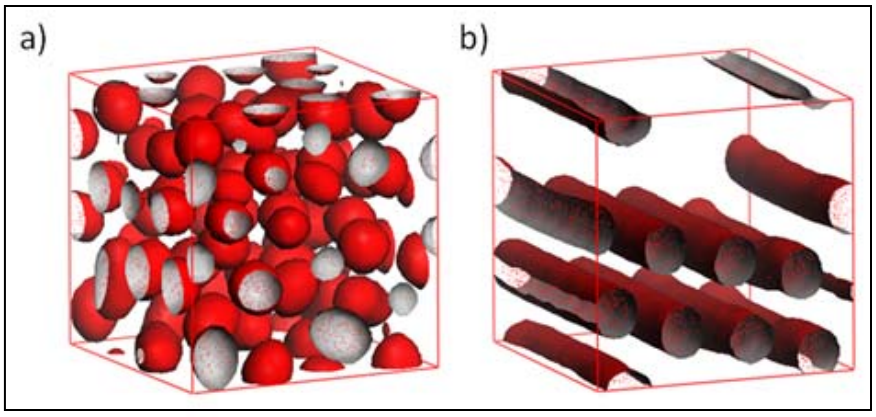

Figure 3. Phase evolution with increasing B homopolymer-solvent length for a 50/50 blend (by volume) of the triblock copolymer and homopolymer-solvent for $\chi_{AB}N = 59.4$ and 73.5, where macrophase separation is observed when the solvent is represented for 5 and 4 beads, respectively. Isosurfaces are shown for the A component (red online), where the B component is excluded for clarity.

This transition has been extensively studied for AB diblock copolymers, where the same general observations can be applied to our triblock copolymer system. When the relative length of the homopolymer-solvent is considerably smaller than the copolymer, corresponding to the solvent limit, it segregates quite evenly between the two phases due to the relatively large translational entropy of the homopolymer-solvent, where the partitioning relieves chain stretching of both blocks at the expense of increased A-B contacts. Once the size of the microdomain is smaller than the undisturbed homopolymer-solvent, constraining it within the microdomains will cause a loss of conformational entropy due to the compressed configuration of the homopolymer-solvent. Instead the homopolymer-solvent demixes from the copolymer and the system macrophase separates into a coexisting ordered and disordered phase formed mostly by the triblock

copolymer and homopolymer-solvent, respectively (*28*, *34–40*). Between these two limits, at intermediate ratios, the translational entropy of the homopolymer-solvent decreases and will segregate into the microdomains formed by the same species in order to reduce the interfacial energy between the two dissimilar species.

Since the B end blocks are constrained to an interface, the mechanical properties of triblock copolymers are different from that of the analogous AB diblock. Triblock copolymers can exhibit a looped or bridged configuration, where the B interface is located at the same interface in the former, while in the latter they reside on different interfaces (*16*, *20*, *41–43*). To calculate elastic properties for our system, we used a finite-element-based mechanical homogenization method for linear elasticity, where the details of the model can be found in references 44 and 45. This method was used to calculate the relative values of the Young's (E) and shear (G) moduli by Andzelm et al. (*44*) for a SIBS triblock copolymer melt and requires two input parameters for each species: the Young's modulus and the Poisson ratio, which were taken to be 3.34 (0.001) and 0.38 (0.499) for the glassy A (rubbery B) phase. The l_2 norm of the Young's and shear moduli for $\chi_{AB}N \approx 73.5$ as a function of Φ are shown in figure 4 for the ordered microphases and were calculated from the components of the moduli ((E_{xx}, E_{yy}, E_{zz}) or (G_{xy}, G_{xz}, G_{yz})) in the transverse (x), vertical (y), and longitudinal (z) directions. In addition, the degree of monotropy, E_{zz}/E_{yy} is plotted as a function of solvent volume fraction, where deviates from unity indicate departure from isotropy. Only one anisotropy factor is needed since $E_{xx} \approx E_{yy}$ for the morphologies considered. Figure 4. The l_2 norm of the (top) Young's and (middle) shear moduli as well as our (bottom) anisotropy factor which we take as the ratio of the Young's modulus in the *z*- and *x*-directions at $\chi_{AB}N = 73.5$ as a function of solvent volume fraction.

indicates that the spherical ($\Phi_s = 0.5–0.6$) morphology is isotropic ($E_{xx} \approx E_{yy} \approx E_{zz}$), while monotropy is observed in the cylindrical ($\Phi_s = 0.1–0.4$) and gyroid phase ($\Phi_s = 0$) ($E_{xx} \approx E_{yy} < E_{zz}$).Since the gyroid phase exhibits cubic symmetry, there should be no directional dependence in the Young's modulus (*46*), and the material is isotropic rather than anisotropic as our calculation suggest. This deviation is due to the defective nature of our structure and our shearing process which promotes anisotropy. In terms of the mechanical properties, the Young's modulus tends to decreases with increasing solvent concentration, indicating a reduction in stiffness and resistance to stretching with dilution. The shear modulus indicates that resistance to volume preserving shear decreases in the following phase sequence: gyroid → spherical → cylindrical. The Young's and shear moduli for the two ordered phases shown in figure 2c and d, were also calculated to be (0.283 GPa, 0.290 GPa, 0.288 GPa) and (0.093 GPa, 0.094 GPa, 0.097 GPa), respectively, for the microphase separated spherical phase and (0.241 GPa, 0.217 GPa, 0.492 GPa) and (0.048 GPa, 0.047 GPa, 0.074 GPa), respectively, for the macrophase separated cylindrical phase. Thus, when the B homopolymer-solvent macrophase separates from the triblock copolymer, the system becomes anisotropic in the *z*-direction, where the system exhibits less resistance to shear compared to the spherical phase.

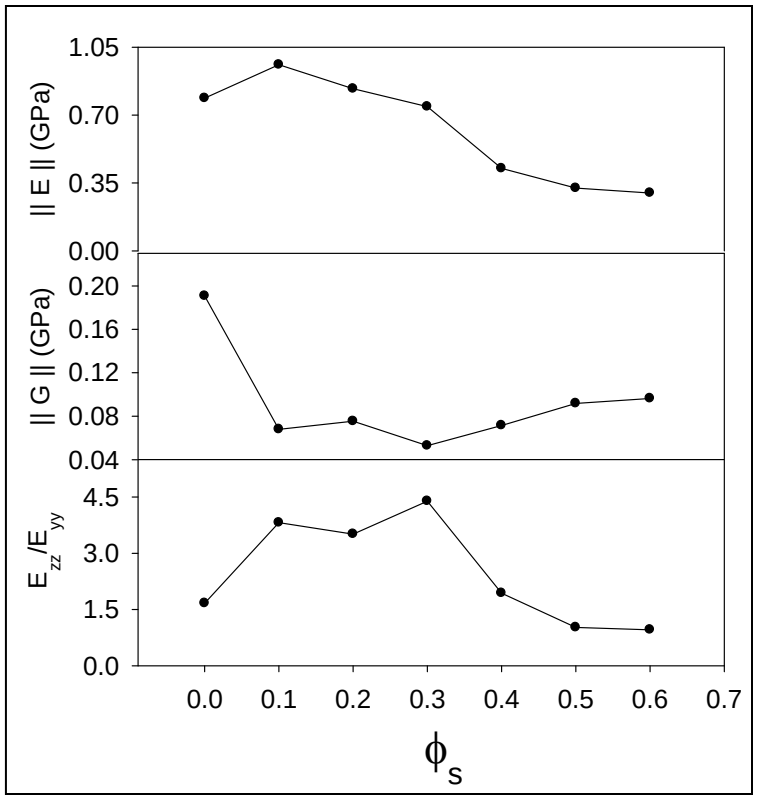

Figure 4. The l_2 norm of the (top) Young's and (middle) shear moduli as well as our (bottom) anisotropy factor which we take as the ratio of the Young's modulus in the *z*- and *x*-directions at $\chi_{AB}N = 73.5$ as a function of solvent volume fraction.

4. Conclusion

In conclusion, we investigated the phase behavior for an $A_3B_{15}A_3$ triblock immersed in a B_1 selective solvent as a function of solvent volume fraction and A-B repulsion in order to model an experimental system composed of poly[styrene-b-(ethylene-co-butylene)-b-styrene] in a midblock selective mineral oil. Solvent swelling of the microdomains modifies the phase behavior from the neat triblock copolymer, where the gyroid phase becomes unstable with small solvent concentrations and the spherical morphology becomes the sole microphase at high dilutions. The effect of solvent length was also studied for a 50/50 (by volume) mixture of copolymer and solvent, where a transition from a microphase to macrophase separated solvent

was observed after a critical length due to the conformational entropy loss associated with confining a long homopolymer-solvent within a relatively compressed microdomain. Finally, elastic properties were calculated using a finite-element-based mechanical homogenization method for the gyroid, cylindrical, spherical, and macrophase separated cylindrical phases.

5. References

1. Bates, F. S. Polymer-Polymer Phase Behavior. *Science* **1991**, *251*, 898–905.
2. Lauer, J. H.; Mulling, J. F.; Khan, S. A.; Soibtaj, R. J.; Bukovnik, R. Thermoplastic Elastomer Gels. I. Effects of Composition and Processing on Morphology and Gel Behavior. *Journal of Polymer Science: Part B: Polymer Physics* **1998**, *36*, 2379–91.
3. Ghosh, S.; Khastgir, D.; Bhowmick, A. K. Phase Modification of SEBS Block Copolymer by Different Additives and Its Effect on Morphology, Mechanical and Dynamic Mechanical Properties. *Journal of Applied Polymer Science* **1997**, *67*, 2015–25.
4. Kim, S. H.; Jo, W. H. A Monte Carlo Simulation for Micellization of ABA- and BAB-type Triblock Copolymers in Selective Solvents. *Macromolecules* **2001**, *34*, 7210–18.
5. Sliozbert, Y. R.; Andzelm, J. W.; Brennan, J. K.; Vanlandingham, M. R.; Pryamitsym, V.; Ganesan, V. Modeling Viscoelastic Properties of Triblock Copolymers: A DPD Simulation Study. *Journal of Polymer Science: Part B: Polymer Physics* **2009**, *48*, 15–25.
6. Bras, R. E.; Shull, K. R. Self-consistent Field Theory of Gelation is Triblock Copolymer Solution. *Macromolecules* **2009**, *42*, 8513–20.
7. van Vlimmeren, B.A.C.; Maurits, N. M.; Zvelindovsky, A.V.M.; Sevink, G.J.A.; Fraaije, J.G.E.M. Simulation of 3D Mesoscale Structure Formation in Concentrated Aqueous Solution of the Triblock Polymer Surfactants (Ethylene Oxide)13(Propylene Oxide)30(Ethylene Oxide)13 and (Propylene Oxide)19(Ethylene Oxide)33(Propylene Oxide)19. Application of Dynamic Mean-Field Density Functional Theory. *Macromolecules* **1999**, *32*, 646–56.
8. Fraaije, J.G.E.M.; van Vlimmeren, B.A.C.; Maurits, N. M.; Postma, M.; Evers, O. A.; Hoffmann, C.; Altevogt, P; Goldbeck-Wood, G.. The Dynamic Mean-field Density Functional Method and its Application to the Mesoscopic Dynamics of Quenched Block Copolymer Melts. *Journal of Chemical Physics* **1997**, *106*, 4260–69.
9. Fraaije, J.G.E.M.; Sevink, G.J.A.; Zvelindovsky, A.V.M. in I.W. Hamley (Ed.), *Developments in block copolymer science and technology*. Wiley, West Sussex, 2003.
10. Materials Studio v. 4.0, Accelrys, San Diego, CA, USA.
11. Horvat, A.; Lyakhova, K. S.; Sevink, G.J.A.; Zvelindovsky, A.V.M.; Magerle, R. Phase Behavior in Thin Films of Cylinder-forming ABA Block Copolymers: Mesoscale modeling. *Journal of Chemical Physics* **2004**, *120*, 1117–26.

12. Zvelindovsky, A.V.M.; Sevink, G.J.A. Sphere Morphology of Nlock Vopolymer Systems Under Dhear. *Europhysics Letters* **2003**, *62*, 370–76.

13. Hildebrand, J. H.; Scott, R. L. *The Solubility of Non-Electrolytes*; Reinhold, New York, 1949.

14. Case, F.; Honeycutt, J. D. Will My Polymers Mix? - Applications of Modeling to Study Miscibility, Compatibility, and Formulation. *Trends in Polymer Science* 1994, 2 259–66.

15. Hamley, I. W. *The Physics of Block Copolymers*; Oxford University Press, Oxford, 1998.

16. Matsen, M. W.; Thompson, R. B. Equilibrium Behavior of Symmetric ABA Triblock Copolymer Melts. *Journal of Chemical Physics* 1999, 111, 7139–46.

17. Frederickson, G. H.; Ganesan, V.; Drolet, F. Field-Theoretic Computer Simulation Methods for Polymers and Complex Fluids. *Macromolecules* **2002**, *35*, 16–39.

18. Matsen, M. W.; Schick, M. Lamellar Phases of a Symmetric Triblock Copolymer. *Macromolecules* **1994**, *27*, 187–92.

19. Hadziioannou, G.; Skoulios, A. Molecular Weight Dependence of Lamellar Structure in Styrene Isoprene Two- and Three-block Copolymers. *Macromolecules* **1982**, *15*, 258–62.

20. Gehlsen, M. D.; Almdal, K.; Bates, F. S. Order-disorder Transition: Diblock versus Triblock Copolymers. *Macromolecules* **1992**, *1992*, 939–43.

21. Matsen, M. W.; Bates, F. S. Block Copolymer Microstructures in the Intermediate-segregation Regime. *Journal of Chemical Physics* **1996**, *106*, 2436–48.

22. Semenov, A. N. Contribution to the Theory of Microphase Layering in Block-copolymer Melts. *Soviet Physics - JETP* **1985**, *61*, 733–42.

23. Matsen, M. W. The sStandard Gaussian Model for Block Copolymer Melts. *Journal of Physics: Condensed Matter* **2002**, *14*, R21–R47.

24. Leiber, L. Theory of Microsphere, Separation in Block Copolmers. *Macromolecules* **1980**, *13*, 1602–17.

25. Sakamoto, N.; Hashimoto, T.; Han, C. D.; Kim, D.; Vaidya, N. Y. Order-order and Order-disorder Transitions in a Polystyrene-block-polyisoprene-block-polystrene Copolymer. *Macromolecules* **1997**, *30*, 1621–32.

26. Kimishima, K.; Koga, T.; Hashimoto, T. Order-order Phase Transition Between Spherical and Cylindrical Microdomain Structure of Block Copolymer. I. Mechanism of the Transition. *Macromolecules* **2000**, *33*, 968–77.

27. Matsen, M. W. Cylinder <-> Sphere Epitaxial Transitions in Block Copolymer Melts. *Journal of Chemical Physics* **2001**, *114*, 8165–73.

28. Janert, P. K.; Schick, M. Phase Behavior of Binary Homopolymer/Diblock Blends: Temperature and Chain Length Dependence. *Macromolecules* **1998**, *31*, 1109–13.

29. Sugimoto, M.; Sakai, K.; Aoki, Y.; Taniguchi, T.; Koyama, K.; Ueda, T. Rheology and Morphology Change with Temperature of SEBS/Hydrocarbon Oil Blends. *Journal of Polymer Science: Part B: Polymer Physics* **2009**, *47*, 955–65.

30. Hanley, K. J.; Lodge, T. P.; Huang, C. I. Phase Behavior of a Block Copolymer in Solvents of Varying Selectivity. *Macromolecules* **2000**, *33*, 5918–31.

31. Suo, T.; Yan, D.; Yang, S.; Shi, A. C. A Theoretical Study of Phase Behaviors in Diblock Copolymers in Selective Solvents. *Macromolecules* **2009**, *42*, 6791–98.

32. Banaszak, M.; Whitmore, M. D. Self-consistent Theory of Block Copolymer Blends: Selective Solvent. *Macromolecules* **1992**, *25*, 3406–12.

33. Lodge, T. P.; Hamersky, M. W.; Hanley, K. J.; Huang, C.I. Solvent Distribution in Weakly-ordered Block Copolymer Solutions. *Macromolecules* **1997**, *30*, 6139–49.

34. Janert, P. K.; Schick, M. Phase Behavior of Ternary Homopolymer/Diblock Blends: Influence of Relative Chain Lengths. *Macromolecules* **1997**, *30*, 137–44.

35. Fytas, G. Effect of Homopolymer Molecular Weight on the Morphology of Block Copolymer/Homopolymer Blends. *Macromolecules* **1987**, *20*, 1431–34.

36. Lee, S. H.; Char, K.; Kim, G. Order-disorder and Order-order Transitions in Mixtures of Higly Asymmetric Triblock Copolymer and Low Molecular Weight Homopolymers. *Macromolecules* **2000**, *33*, 7072–83.

37. Whitmore, M. D.; Noolandi, J. Theory of Micelle Formation in Block Copolymer-Homopolymer Blends. *Macromolecules* **1985**, *18*, 657–65.

38. Jeon, K. .; Roe, R. J. Solubilization of a Homopolymer in a Block Copolymer. *Macromolecules* **1994**, *27*, 2439–47.

39. Roe, R. J.; Zin, W. C. Phase Equilibria and Transition in Mixtures of a Homopolymer and a Block Copolymer. 2. Phase diagram. *Macromolecules* **1984**, *17*, 189–94.

40. Baek, D. M.; Han, C.D.; Kim, J. K. Phase Equilibria in Mixtures of Block Copolymer and Homopolymer. *Polymer* **1992**, *33*, 4821–31.

41. Adams, J.L.; Graessley, W.W.; Register, R.A. Rheology and the Microphase Seperation in Styrene-Isoprene Block Copolymers. Macromolecules 1994, 27.

42. Mckay, K. W.; Gros, W. A.; Diehl, C. F. The Influence of Styrene-butadiene Diblock Copolymer on Styrene-butadine-styrene triblock Copolymer Viscoelastic Properties and Produce Performance. *Journal of Applied Polymer Science* **1995**, *56*, 947–58.

43. Riise, B. L.; Fredrickson, G. H.; Larson, R. G. Pearson, D. S. Rheology and Shear-induced Alignment of Lamellar Diblock and Triblock Copolymers. *Macromolecules* **1995**, *28*, 7653–59.

44. Andzelm, J. W.; Beyer, F. L.; Snyder, J.; Chung, P. W. Multiscale Simulations of Triblock Copolymers. *International Journal of Multiscale Computational Engineering* **2007**, *5*, 167–79.

45. Chung, P. W.; Tamma, K. K.; Namburu, R. R. Asymptotic Expansition Homogenization for Heterogeneous Media: Computational Issues and Applications. Composites Part A. *Applied Science and Manufacturing* **2001**, *32*, 1291–301.

46. Hajduk, D. A.; Harper, P. E.; Gruner, S. M.; Honeker, C. C.; Kim, G.; Thomas, E. L.; Fetters, L. J. The Gyroid: A New Equilibrium Morphology in Weakly Segregated Diblock Copolymers. *Macromolecules* **1994**, *27*, 4063–75.

List of Symbols, Abbreviations, and Acronyms

ARL	U.S. Army Research Laboratory
C_{14}	hydrocarbon oil tetradecane
DDFT	dynamic density functional theory
DoD	Department of Defense
MS	Material Studios
ODT	order-disorder transition
SBS	poly[styrene-butadiene-styrene]
SCFT	self-consistent field theory
SEBS	poly[styrene-(ethylene-co-butylene)-styrene]
SIBS	poly[styrene-isobutylene-styrene]
SIS	poly[styrene-isoprene-styrene]
TPE	thermoplastic elastomer

1 PDF DEFENSE TECH INFO CTR
ATTN DTIC OCA (PDF)
8725 JOHN J KINGMAN RD STE 0944
FT BELVOIR VA 22060-6218

20 US ARMY RSRCH LAB
ATTN RDRL WMM G T CHANTAWANSRI (20 COPIES)
BLDG 4600 RM C228
ABERDEEN PROVING GROUND MD 21005

1 US ARMY RSRCH LAB
ATTN RDRL CIM G T LANDFRIED
BLDG 4600
ABERDEEN PROVING GROUND MD 21005-5066

3 US ARMY RSRCH LAB
ATTN IMNE ALC HRR MAIL & RECORDS MGMT
ATTN RDRL CIM L TECHL LIB
ATTN RDRL CIM P TECHL PUB
ADELPHI MD 20783-1197

TOTAL: 25 (1 PDF, 24 HCS)